



# Responses of Human Osteosarcoma Cells to Hydroxyapatite Nano-Particles on TiO<sub>2</sub> Surfaces; an *In-Vitro* Study

TN Premachandra<sup>1\*</sup>; WPSL Wijesinghe<sup>2</sup>; RPVJ Rajapakse<sup>1</sup>; RMG Rajapakse<sup>2</sup>; CNRA Alles<sup>3</sup>; HMTU Herath<sup>4\*</sup>

<sup>1</sup>Department of Veterinary Pathobiology, Faculty of Veterinary Medicine and Animal Science, University of Peradeniya, Sri Lanka.

<sup>2</sup>Department of Chemistry, Faculty of Science, University of Peradeniya, Sri Lanka.

<sup>3</sup>Department of Biochemistry, Faculty of Medicine, University of Peradeniya, Sri Lanka.

<sup>4</sup>Department of Medical Laboratory Science, Faculty of Allied Health Science, University of Peradeniya, Sri Lanka.

## \*Corresponding Author(s): HM Thushari Uthpala Herath

Department of Medical Laboratory Sciences, Faculty of Allied Health Sciences, University of Peradeniya.

E-mail: uthpalath@yahoo.com

## Thejane Nisansala Premachandra

Department of Veterinary Pathobiology, Faculty of Veterinary Medicine and Animal Science, University of Peradeniya, Sri Lanka.

E-mail: thejaninisa@gmail.com

## Abstract

Fabricated Hydroxyapatite (HA) nano-particles that mimic natural HA are extensively used as coatings on prostheses to repair, renovate and replace human bones. However, the attainability of these materials is limited for developing countries due to the high cost of both raw materials and material processing. Therefore, Wijesinghe et al. (2014), have produced natural HA nano-particles through atomized spray pyrolysis technique and have successfully prepared Ti surfaces with a binder TiO<sub>2</sub> layer coated with locally synthesized HA nano-particles, which would be a simple material with high economic value for orthopedics applications. Therefore, with the intension of assessing the suitability in the fabrication of orthopaedic implants, this novel material was evaluated for cytotoxicity and biocompatibility *in-vitro* using osteoblast-like cells. The results of this study demonstrate, the surfaces of Ti with TiO<sub>2</sub> thin layer, coated with locally synthesized HA does not elicit any toxic effect to cells and encourage cell adhesion when in contact with the material surfaces. Furthermore, HOS cells adhered to the material surfaces preserve their characteristic morphology while maintaining their osteoblast phenotype and undergoing developmental stages leading to mineralization, successfully.

In conclusion, this material will be a promising candidate in the production of low cost synthetic orthopaedic implants having a great potential in advancement of orthopaedic applications.

Received: Dec 21, 2021

Accepted: Feb 17, 2022

Published Online: Feb 22, 2022

Journal: Journal of Nanomedicine

Publisher: MedDocs Publishers LLC

Online edition: <http://meddocsonline.org/>

Copyright: © Herath HMTU & Premachandra TN (2022).

This Article is distributed under the terms of Creative Commons Attribution 4.0 International License

**Keywords:** Cell Culture; Osteoblast; Hydroxyapatite; Biocompatibility.

**Cite this article:** TN Premachandra, WPSL Wijesinghe, RPVJ Rajapakse, RMG Rajapakse, CNRA Alles. Responses of Human Osteosarcoma Cells to Hydroxyapatite Nano-Particles on TiO<sub>2</sub> Surfaces; an In-Vitro Study. J Nanomed. 2022; 5(1): 1053.



## Introduction

Bone tissue is the hardest tissue in the body, which differs greatly from others. Collagen matrix and inorganic component, calcium phosphate are the two main components responsible for this characteristic hardness. The role of bone lining osteoblasts seems to play an important part in coupling bone resorption to bone formation. Among these, active osteoblasts are accountable for bone development originating from immature mesenchymal stem cells [1].

Bone defects and disabilities are common consequences of the explosions of land mines and other explosive devices during war battles, accidental injuries, traumas and non-traumatic disorders such as cancers. In most of the instances particularly, part of the bone or complete bone with the joint is damaged, necessitating replacement or reconstruction to stabilize movements and restore the function of affected part of the body. Surgical treatment involves the implantation of bone bonding materials into bone defects, which will enhance patient's quality of life.

At present, when compared to other materials used to manufacture orthopedic implant materials, metallic biomaterials are mostly used to correct bone defects, due to their high fracture toughness and high tensile strength. However, surface modification of these materials is usually required to decrease corrosion, to improve bioactivity and osteo-integration [2]. Synthetic Hydroxyapatite (HA)  $[\text{Ca}_{10}(\text{PO}_4)_6(\text{OH})_2]$  which mimics natural HA has been extensively used as biocompatible coatings [3,4]. Currently, there are several techniques to coat Ti surfaces with HA such as dip-coating method, sol-gel methods, sputter-coating, template assisted electro hydrodynamic atomization, electrophoretic deposition, thermal spraying, pulsed laser ablation and dynamic mixing [2,5-8].

However, most of these methods are linked with certain inherent drawbacks; low bonding strength at  $\text{TiO}_2$  and HA interface, uneven surfaces as well as uncontrollable coating thickness and decomposition of HA into other calcium phosphates [9,10]. Furthermore, due to high cost, the implants made out of such materials are not always accessible to many patients in developing countries [11]. Therefore, development of low-cost coating techniques is essential to overcome such draw backs. In order to address this issue Bandara et al. (2011) have designed and developed a novel technique based on Atomized Spray Pyrolysis (ASP) to fabricate uniform layers of interconnected nano-particles on substrates which is simple and cost effective [12]. One of its major advantages is the ability to use readily and freely available and inexhaustible atmospheric oxygen, which gives a uniform and phenol-free  $\text{TiO}_2$  coating on Ti. Accordingly, they have successfully introduced Ti surfaces with a binder  $\text{TiO}_2$  identified as Surface Modified Ti Metal (SMTiM) coated with a HA layer [8].

In the current study, Ti samples with self formed  $\text{TiO}_2$  thin layer coated with locally synthesized HA nano-particles were prepared by atomized spray pyrolysis and the feasibility of using those surfaces in orthopaedic applications was evaluated. Biological responses of human osteoblast-like cells (HOS, ATCC, CRL 1543) [13] to HA surfaces were observed *in vitro* allowing a more direct vision of the biological response and cell-material interaction under controlled conditions.

## Materials and methods

HA nano-particles have been synthesized under calcium su-

crate route where the method has been described elsewhere [8,12,14]. In order to prepare phenol free titanium dioxide binder layer, cleaned Ti metal pieces have been subjected to heat treatment and followed by introducing HA coating using atomized spray pyrolysis system. Proper attachment of HA on Ti surfaces has been ensured through a second heat treatment at 700 °C for 3 hours [12].

The morphology of test samples was analyzed by Scanning Electron Microscopy (SEM, Zeiss, German). The elemental composition of prepared HA samples was analyzed by Energy-Dispersive X-ray (EDX) spectroscopic (Oxford, UK). The samples were sterilized by gamma irradiation (Co 60, 25 KGy) before using for *in vitro* studies.

Human Osteosarcoma Cells (HOS, ATCC, CRL 1543) were cultured in Dulbecco's Modified Eagle's Medium (DMEM) (Sigma, USA), supplemented with 10% Fetal Calf Serum (FCS), 1% non-essential amino acids, 150 µg/ml ascorbic acid, 0.02 mM L-glutamine, 0.01 M HEPES (4-(2-hydroxyethyl)-1-piperazineethanesulfonic acid), penicillin (100 units/ml) and streptomycin (100 units/ml). Thermanox™ cover slips (TMX, NUNC™, USA) and absolute ethanol were used as the tissue culture control and positive toxic control, respectively. HOS cells were seeded at a density of  $2 \times 10^6$  cells/ml on test and control samples for proliferation and differentiation studies. The culture plates were incubated at 37 °C in a humidified air supplied with 5%  $\text{CO}_2$  for 1, 7, 14, 21, 28 and 35 days. The culture medium was replaced at intervals, minimizing disturbances to culture conditions.

Duplicate samples for each time point were prepared for SEM analysis by seeding cells at a density of  $2 \times 10^5$  cells ml<sup>-1</sup> and were incubated at 37 °C in humidified air with 5%  $\text{CO}_2$ . After 24 h, 48 h and 168 h of incubation, the cultures were fixed with 1.5% glutaraldehyde in 0.1 M sodium cacodylate, stained in 1% osmium tetroxide in 0.1 M sodium cacodylate and 1% tannic acid buffer and dehydrated using a series of aqueous alcohol solutions starting from 20%-70% in 10% increments. The surfaces were stained with 0.5% uranyl acetate and further dehydrated in 90%, 96% and 100% ethyl alcohol containing  $\text{Na}_2\text{CO}_3$  and with hexamethyl-di-salazane and finally air dried. The sample surfaces were coated with gold for examination under scanning electron microscope (Zeiss, German) to observe morphology of cells attached to materials surfaces.

The cytotoxicity and viability of cells once attached to the test material were determined by performing MTT (3-(4,5 dimethylthiazol 2-yl)-2,5-diphenyltetrazolium bromide) assay. Extracts were prepared by incubating test samples in complete DMEM at 37 °C for 1, 7, 14, 21, 28 and 35 days. HOS cells were cultured in the extracts at 37 °C in a humidified air at 5%  $\text{CO}_2$  for 24 h and for further 4 h in the presence of 10% MTT (Sigma, USA). Dimethyl Sulfoxide (DMSO) was added after removing the medium and was placed on a shaker (Themofisher, UK) for 10 min to ensure complete dissolution of crystals. Absorbance was measured at 570 nm and emission at 620 nm (Multiskan EX, Thermo, China). The results were presented from 8 replicates of 3 experiments at each time point.

HOS cells were cultured on material surfaces at  $2 \times 10^6$  cells/ml density and was incubated at 37 °C in humidified air with 5%  $\text{CO}_2$  for 1, 7, 14, 21, 28 and 35 days to evaluate cell proliferation. The used culture medium was replaced at pre-determined time intervals. One milliliter of 10% alamar Blue™ (Sigma, USA), in phenol-red free medium was added to each well and was incubated at 37 °C in a humidified air at 5%  $\text{CO}_2$  for 4 h. The absor-

balance was read at 570 nm with a reference wavelength of 630 nm (Multiskan EX, Thermo, China). The procedure was done in triplicate for both test and control materials. All the wells were replaced with fresh DMEM after washed with PBS and were further incubated. This procedure was carried out serially for 1, 7, 14, 21, 28 and 35 days of incubation.

In order to determine the total DNA content, cells were lysed at each pre-decided time intervals; namely, day 1, 7, 14, 21, 28 and 35, using freeze/thaw cycle [4 cycles  $\times$  (-70 °C for 20 min / 37 °C for 20 min)]. Total DNA was extracted using taco mini DNA extraction machine (POKIT, GeneReach Biotechnology, Taiwan) and was measured using Qubit 2.0 fluorometer (Thermo Fisher, USA). The results were obtained from 2 replicates of 2 experiments for each time point.

Bicinchoninic Acid Protein Assay was performed to determine the total protein content. Cells were lysed at each time point (i.e. days 1, 7, 14, 21, 28 and 35) using freeze/thaw cycle [4 cycles  $\times$  (-70 °C for 20 min / 37 °C for 20 min)]. The protein standards in Bicinchoninic Acid Protein Assay kit were used to obtain the standard curve with a concentration range of 0, 2, 4, 6, 8, 10  $\mu$ g/ml. The amount of protein present in the samples was determined using the standard curve. Fluorescence was measured on a plate reader (Multiskan EX, Thermo, China) at a wavelength of 560 nm. The results were presented from 2 replicates of 2 experiments at each time point.

ALP is an early marker of osteoblast phenotype [15]. ALP activity of cells, lysed at pre-determined time point (i.e. days 1, 7, 14, 21, 28 and 35) using freeze/thaw cycle [4 cycles  $\times$  (-70 °C for 20 min / 37 °C for 20 min)] was measured using QuantiChrome™ Alkaline Phosphatase Assay Kit (Bio Assay Systems, USA, Catalog No. DALP-250).

The production of osteocalcin was determined using Anti - osteocalcin antibody (bone gamma-carboxyglutamate (gla) protein, Rabbit IgG, Booster biotechnology, USA). For the detection of the expression of osteocalcin by immunofluorescence,  $2 \times 10^5$  cells were seeded on the test sample surfaces and the negative (Thermanox™) control. At each time point (i.e. day 1, 7, 14, 21, 28 and 35) cells were washed with PBS and then fixed in 4% paraformaldehyde for 15 min and permeabilized with 1% Triton X-100 in PBS for 5 min. The background was blocked with 5% bovine serum albumin for 15 min and incubated with primary antibody (bone gamma-carboxyglutamate (gla) protein, Rabbit IgG, Booster biotechnology, USA) for 1h at room temperature and then cells were again incubated with flurophore conjugated secondary antibody for 1h, which was counter stained with Ethidium Bromide. Cells were observed by fluorescence microscopy (Zeiss, Scope A1, Germany).

In order to determine the mineralization of matrix HOS cells were cultured on materials surfaces at a density of  $2 \times 10^6$  cells/ml and were incubated for 48 days at 37 °C in humidified incubator with 5% CO<sub>2</sub>. Sample surfaces were washed in distilled water and covered with 1 ml of 2 % silver nitrate. Those were then exposed to bright sun light for 20-60 min and again washed with three changes of distilled water. Samples were treated with 2.5% sodium thiosulphate for 2 min. Samples were blot dried after washing under running water and were examined under the microscope (Zeiss, Scope A1, Germany).

Furthermore, after 48 days of incubation, the cultures seeded with same density of cells were fixed with 1.5% glutaraldehyde in 0.1 M sodium cacodylate, stained in 1% osmium tetrox-

ide in 0.1 M sodium cacodylate. The elemental composition of HA surfaces after were analyzed using EDX (Oxford, UK) to detect the presence of Ca on the cell layer grown on HA surfaces.

Statistical analysis was done by student 't' test using Graph-Pad Prism 5 for windows (GraphPad software, USA, 95% confidence level) software.

## Results and discussion

### Characterization of synthesized HA products

The SEM image of the surfaces coated with HA synthesized at 700 °C clearly shows the nanometer size HA particles on SMTiM surfaces (Figure1). The initial rod-like HA nanoparticles have been converted to spherical HA while sintering at high temperatures (700 °C) as described elsewhere [14]. Presence of Ca and P on materials surfaces was clearly depicted in the EDX spectrum (Figure 2).

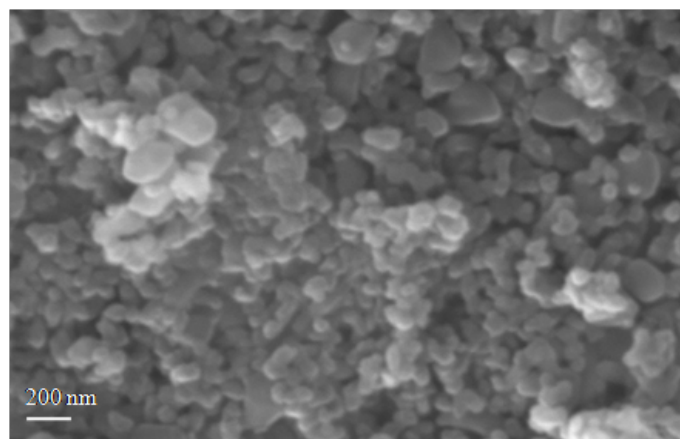


**Figure 1:** The SEM images of the hydroxyapatite samples, after subjecting to calcination at 700 °C for 3 h.

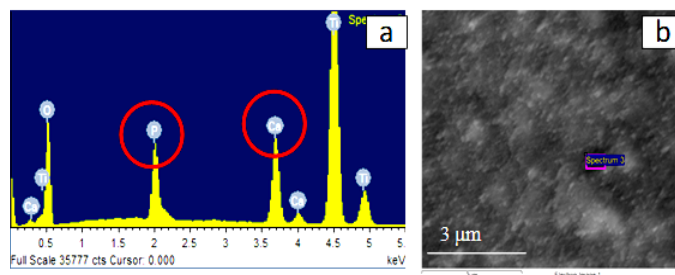


**Figure 2:** (a) EDX spectrum and (b) SEM image of HA coated on SMTiM surfaces.

### Cell morphology and attachment

Cells attached to material surfaces maintained the usual polygonal morphology [16] with few exceptions resulting as a response to surface characteristics. HOS cells attached to the Thermanox™ control were stretched across the surfaces with extended cytoplasmic process after 24 h. Lamellipodia attached to HA surface (Figure 3a) made the cells flat and evenly spread (Figure 3b). The rounded cells present which may be undergoing cell division can be interpreted as an indication of cell proliferation (Figure 4a and b). Material surfaces devoid of cells were observable at 24 h while cells showed confluent growth after 48 h of incubation indicating the presence of favorable environment which provides survivability of cells on the HA surfaces (Figure 4a). The cell margins were merged and it was difficult to define their boundaries and the underlying material was cov-

ered with cells. The cells spread on all the surfaces became confluent and were closely attached to the surfaces after 168 hours of incubation (Figure 5a) making a continuous sheath over the surfaces making it difficult to identify cell margins (Figure 5b).

According to the SEM images the HA surfaces have favored cell adhesion and were able to support normal osteoblast growth. Cell adhered with well extended filopodia along the surfaces is an indication for favourable cell attachment.

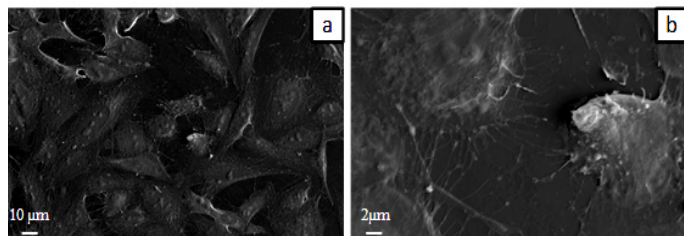


**Figure 3:** SEM images of cells on HA surface after 24 h incubation at two different magnifications. (a) Closely packed cell layer on the HA surface (1.00 K X), (b) The terminal ends of extended filopodia (5.00 K X).

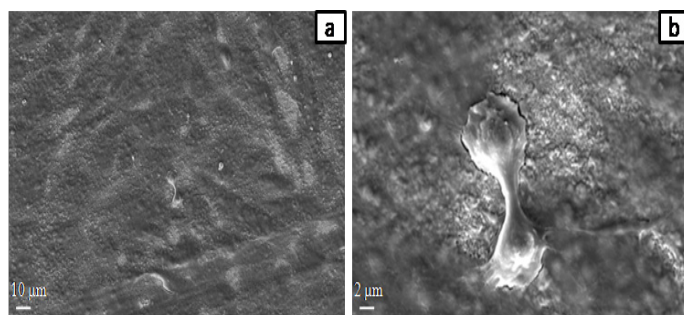


**Figure 4:** SEM images of cells on HA surface after 48h incubation at two different magnifications. (a) A dense layer of confluent HOS cells on HA surface (1.00 K X), (b) Cell in the process of cell division (5.00 K X).

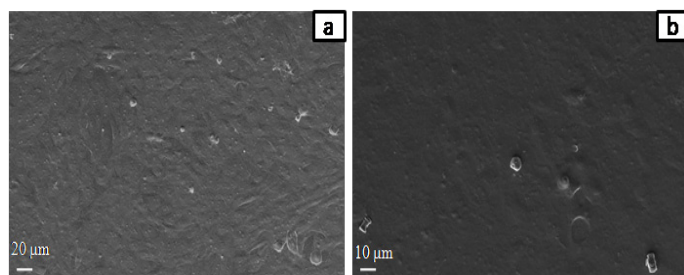


**Figure 5:** SEM images of cells on HA surface after 48h incubation at two different magnifications. (a) A dense layer of confluent HOS cells on HA surface (1.00 K X), (b) Cell in the process of cell division (5.00 K X).

**Evaluation of cytotoxicity**

MTT [3-(4, 5-Dimethylthiazol-2-yl)-2, 5-Diphenyltetrazolium Bromide] assay is a rapid and versatile colorimetric assay, based on the tetrazolium salt. MTT measures living cells quantitatively while the tetrazolium ring is cleaved by active mitochondria [17]. According to Mosmann [18] MTT is cleaved by all living and metabolically active cells but not by dead cells.

According to the results of MTT assay a significant difference was observed between test samples and the positive toxic control ( $p < 0.001$ ) indicating that HA prepared locally was not toxic to the cell membrane (Figure 6).

Interestingly, the results of the sample elutions were comparable to that of the negative control (DMEM + 10% FCS) reaching the maximum level at day 1 and decreasing thereafter and reaching a consistent level after day 14 till the end of the study period. Results of the MTT assay confirm that these materials were non toxic to cell membranes and the materials did not elicit any substance that would bring deleterious effect to cells.

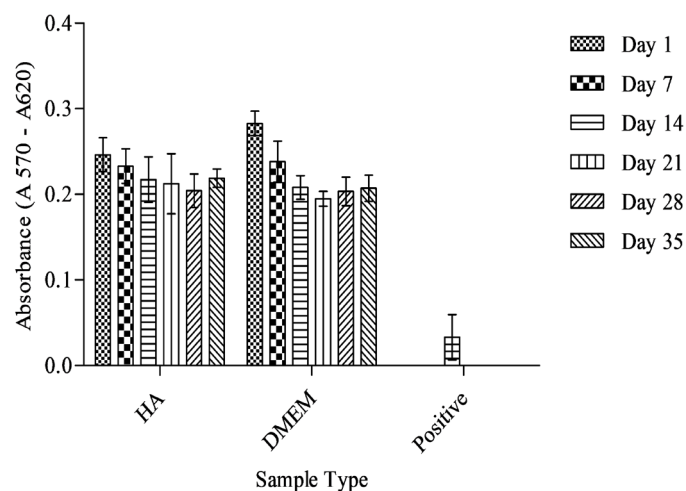


**Figure 6:** SEM images of cells on HA surface after 48h incubation at two different magnifications. (a) A dense layer of confluent HOS cells on HA surface (1.00 K X), (b) Cell in the process of cell division (5.00 K X).

**Growth and proliferation of cells on HA coated SMTiM**

Proliferation was determined using alamarBlue™ assay. AlamarBlue™ is a redox indicator, which can be used to measure proliferation quantitatively [19]. The metabolic activity of cells grow in culture, maintains a reducing environment in the surrounding culture medium, while growth inhibition produces an oxidising environment [17,19,20]. This reducing environment causes Colour change of alamarBlue™ indicator from non-fluorescent (blue) to fluorescent (red). According to the test results, a consistent increase in proliferation of cells attached to the surface of test samples was observed up to day 14 (Figure 7). This pattern was comparable to that of the TMX control; a significant increase in cell proliferation was observed on both the test material and the TMX in comparison to the positive toxic control ( $p < 0.001$ ). Hence, the results demonstrate that HA surfaces promoted initial as well as long-term osteoblast-like cell proliferation.

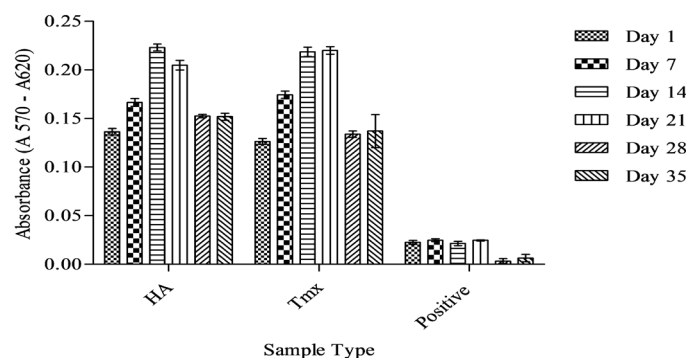


**Figure 7:** AlamarBlue™ assay for HOS cell proliferation for HA coated on SMTiM surfaces, negative (TMX) and positive (alcohol) controls (Arithmetic means, error bars represent 95% confidence intervals and n= 8).

positive (alcohol) controls (Arithmetic means, error bars represent 95% confidence intervals and n= 8).

The results obtained by metabolic assays such as Alamar-blue™ to measure cell proliferation can be further supported by determining the DNA content [21]. Result of the total DNA content of cells was in accordance with those of cell proliferation (Figure 8). Moreover, a gradual increase in total DNA content was observed until day 21 of the cells attached to the test materials and the negative control, TMX. The pattern of the test samples was similar to that of TMX control confirming the fact that test samples did support cell proliferation similar to the tissue culture control. According to the result of the alamarBlue™ and DNA assays it can be concluded that all treated sample surfaces have promoted cell proliferation throughout the study period.

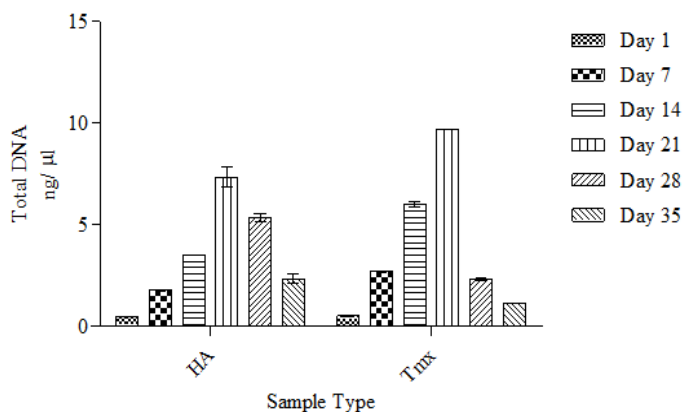


**Figure 8:** Total DNA of cells attached to HA coated on SMTiM surfaces samples and negative (TMX) (Arithmetic means, error bars represent 95% confidence intervals and n= 8).

A gradual increase in total protein content was observed until day 21 of the cells attached to the negative TMX control and until day 35 for the test material (Figure 9). A gradual increase in total protein contents of the cells attached to the test material was seen until end of the study period. It is possible however, that the increased protein content levels observed may be a sign of additional protein adsorption onto the test material from the culture medium. The first event to occur at the cell-implant interface is protein adsorption and hence this feature may be advantageous for subsequent cell adhesion once implanted to the body [22].

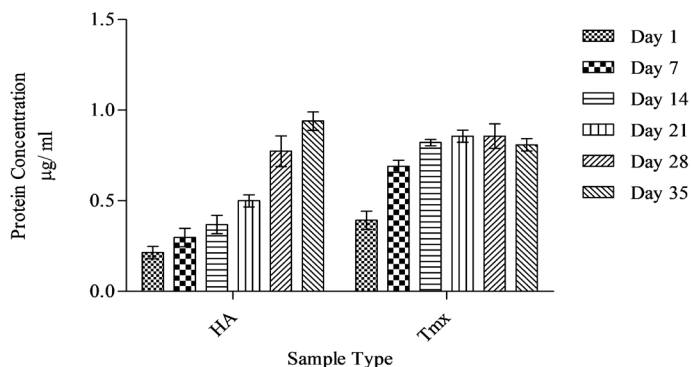


**Figure 9:** Total Protein content of cells attached to the HA coated on SMTiM surfaces and negative (TMX). (Arithmetic means, error bars represent 95% confidence intervals and n= 8).

### Differentiation of cells

The expression of Alkaline Phosphatase (ALP), an early marker of osteoblast cell differentiation [15,17] was detected in the early stages of cells on all test surfaces. ALP activity was used as an indicator of expression of phenotype of the HOS cells. In the present study, the levels of ALP activity reached maxima by day 21 which is comparable to that of the TMX indicating onset of differentiation (Figure10). It has been demonstrated that a decrease in cell proliferation has usually concurred with an increase of differentiation [23]. Confirming this fact, the results demonstrated that differentiation of osteoblast-like cells was initiated by day 21 with a slowing down in cell proliferation.

In the current study osteocalcin, a late marker of osteoblast differentiation and an early indicator of mineralization were detected once the ALP activity reached the maximum levels (Figure 11).

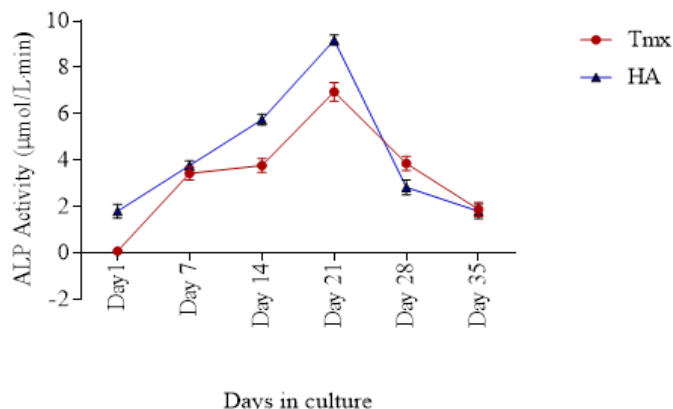


**Figure 10:** Expression of ALP activity of cells attached to the HA coated on SMTiM surfaces and negative (TMX) showing maximum activity by day 21. (Arithmetic means, error bars represent 95% confidence intervals and n= 8).

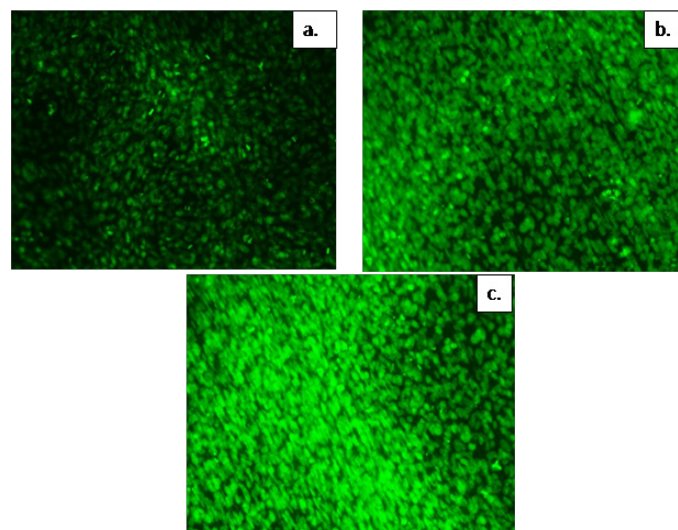


**Figure 11:** Immunofluorescence stain of HOS cells attached to the HA coated on SMTiM surfaces and negative (TMX). a) after 14 days, b) after 21 days, c) after 28 days showing increase production of osteocalcin towards the later part of the study period.

Furthermore, the increase in osteocalcin is a characteristic testing of normal osteoblast growth and differentiation [24]. This matrix protein, which is strongly associated with the mineral phase of bone, is usually produced at a later stage, typically after ALP activity has been detected [25]. A promising justification could be the strong affinity of osteocalcin to hydroxyapatite, leading to onset of bone formation and mineralization.

The results of the current study indicate that cells attached to all the HA surfaces were able to produce osteocalcin there by indicating onset of mineralization which would be followed by bone nodule formation. The EDX spectrum clearly indicates the presence of Ca on the cellular surfaces, which also supports the findings of osteocalcin, indicating (Figure 12) onset of nodule formation and mineralization. These results are well correlated with those of Von Kossa staining, further confirming the onset of mineralization on HA surfaces (Figure 13). This proves the ability of HA surfaces to promote nodule formation without any supplements used to enhance bone formation.

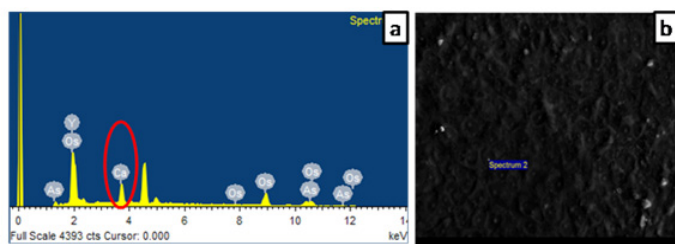


**Figure 12:** (a) EDX spectrum of sample surface entirely covered with cells showing a peak for calcium and (b) SEM image of HOS cell confluence on HA surfaces covering entire surface after 48 days.

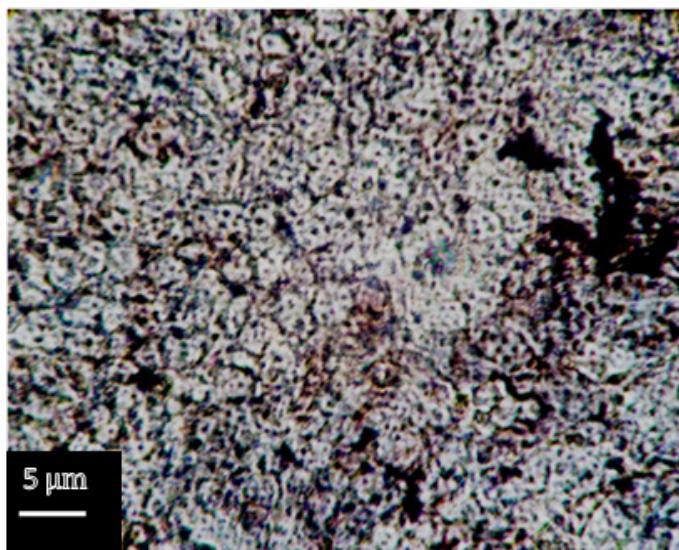


**Figure 13:** Mineralized nodule subjected to von kossa staining on HA surface after 48 days of incubation (optical: Oil immersion).

## Conclusion

The success of any implant material is governed by many factors including the material surface and cell responses, which support effective osseointegration and long-term stability. This study demonstrates that the test material, locally synthesized HA nano-particles coated SMTiM does not show any toxicity to osteoblast-like cells whereas it encourages rapid cell adhesion and enhanced cell proliferation leading to differentiation, providing normal development of cells once attached to the mate-

rial surfaces. All cells attached on the material maintained their typical morphology. Expression of early and late markers for osteoblast function confirmed the maintenance of osteoblast phenotype on HA surfaces while indicating the onset of mineralization. Further, material surfaces support nodule formation, which is an indication for bone formation. In conclusion, this material will be a competent candidate for the production of synthetic bone substitutes with high potential for future developments for load bearing prostheses as well as non-load bearing orthopaedic applications.

## Author contributions

The manuscript was written through contributions of all authors. All authors have given approval to the final version of the manuscript.

## Funding sources

National Research Council, Sri Lanka (NRC 15-027). The Royal Society of UK (International Exchange Scheme 2013/R2).

## References

1. Bassi A, Gough J, Zakikhani M, Downes S. Bone tissue regeneration, *Biomaterials*. 2011; 93-110.
2. Hanawa T. Biofunctionalization of titanium for dental implant, *Jpn Dent Sci Rev*. 2010; 46: 93-101.
3. Gopi D, Indira J, Kavitha L. A comparative study on the direct and pulsed current electrodeposition of hydroxyapatite coatings on surgical grade stainless steel, *Surf. Coat. Technol*. 2012; 206: 2859-2869.
4. Chakraborty J, Daneu N, Recnik A, Chakraborty M, Dasgupta S, et al. Stepwise formation of crystalline apatite in the biomimetic coating of surgical grade SS 316L substrate: A TEM analysis, *J Taiwan Inst Chem Eng*. 2011; 42: 682-687.
5. Mohseni E, Zalnezhad E, Bushroa AR. Comparative investigation on the adhesion of hydroxyapatite coating on Ti-6Al-4V implant: a review paper, *Int J Adhes Adhes*. 2014; 48: 238-257.
6. Surmenev RA. A review of plasma-assisted methods for calcium phosphate-based coatings fabrication, *Surf. Coat. Technol*. 2012; 206: 2035-2056.
7. Balamurugan A, Balossier G, Michel J, Ferreira JMF. Electrochemical and structural evaluation of functionally graded bio-glass-apatite composites electrophoretically deposited onto Ti6Al4V alloy, *Electrochim. Acta*. 2009; 54: 1192-1198.
8. Wijesinghe WPSL, Mantilaka MMMGPG, Senarathna KGC, Herath HMTU, Premachandra TN, et al. Preparation of bone-implants by coating hydroxyapatite nanoparticles on self-formed titanium dioxide thin-layers on titanium metal surfaces, *Mater. Sci. Eng. C*. 2016; 63: 172-184.
9. Wang Q, Zhou FI, Zhou Z, Wang C, Zhang W, et al. Effect of titanium or chromium content on the electrochemical properties of amorphous carbon coatings in simulated body fluid, *Electrochim. Acta*. 2013; 112: 603-611.
10. Simkaa W, Krzakala A, Korotin, DM, Zhidkov IS, Kurmaev EZ, et al. Modification of a Ti-Mo alloy surface via plasma electrolytic oxidation in a solution containing calcium and phosphorus, *Electrochim. Acta*. 2013; 96: 180-190.
11. Yildirim OS, Aksakal B, Celik H, Vangolu Y, Okur A. An investigation of the effects of hydroxyapatite coatings on the fixation strength of cortical screws, *Med Eng Phys*. 2005; 27: 221-228.

12. Bandara HMN, Rajapakse RMG, Murakami K, Kumara GRRA, Sepalage GA. Dye-sensitized solar cell based on optically transparent TiO<sub>2</sub> nanocrystalline electrode prepared by atomized spray pyrolysis technique, *Electrochim. Acta.* 2011; 56: 9159-9161.
13. Clover J, Gowen M. Are MG-63 and HOS TE85 human osteosarcoma cell lines representative models of the osteoblastic phenotype, *Bone.* 1994; 15: 585-591.
14. Wijesinghe WPSL, Mantilaka MMMGPG, Premalal EVA, Herath HMTU, Mahalingam S, Edirisinghe M, et al. Facile synthesis of both needle-like and spherical hydroxyapatite nanoparticles: effect of synthetic temperature and calcination on morphology, crystallite size and crystallinity, *Mater. Sci. Eng. C.* 2014; 42: 83-90.
15. Marom R, Shur I, Solomon R, Benayahu D. Characterization of adhesion and differentiation markers of osteogenic marrow stromal cells, *J. Cell. Physiol.* 2005; 202: 41-48.
16. Di Silvio L, Cellular responses to Biomaterials, first ed., London, England. 2009.
17. Herath HMTU, Di Silvio L, Evans JRG. Osteoblast response to zirconia surfaces with different topographies, *Mater. Sci. Eng. C.* 2015; 363-370.
18. Mosmann T. Rapid colorimetric assay for cellular growth and survival application to proliferation and cyto-toxicity assays, *J. Immunol. Methods.* 1983; 55-63.
19. Nakayama GR, Caton MC, Nova MP, Parandoosh Z. Assessment of the Alamar Blue assay for cellular growth and viability in vitro, *J. Immunol. Methods.* 1997; 204: 205-208.
20. Nociari MM, Shalev A, Benias P, Russo C. A novel one-step, highly sensitive fluorometric assay to evaluate cell-mediate cytotoxicity, *J. Immunol. Methods.* 1998; 213: 157-167.
21. Quent VMC, Loessner D, Friis T, Reichert JC, Hutmacher DW. Discrepancies between metabolic activity and DNA content as tool to assess cell proliferation in cancer research, *J Cell Mol Med.* 2010; 4: 1003-1013.
22. Collier TO, Jenney CR, DeFife KM, Anderson JM. Protein adsorption on chemically modified surfaces, *Biomed. Sci. Instrum.* 1997; 33: 178-183.
23. Nijweide PJ, Burger EH, Feyen JHM. Cells of bone: Proliferation, differentiation and hormonal regulation, *Physiol. Rev.* 1986; 66: 855-886.
24. Boskey AI. Non-collagenous matrix proteins and their role in mineralization. *J. Bone Miner.* 1989; 6: 111-123.
25. Herath HMTU, Di Silvio L, Evans JRG. Biological evaluation of solid free formed hard tissue scaffolds for orthopaedic applications, *J. Appl. Biomater. Funct.* 2010; 8: 89-96.